An MC-SCF Study of [1,3] and [1,2] Sigmatropic Shifts in Propene

Fernando Bernardi,[1a] Michael A. Robb,[†,1b] H. Bernhard Schlegel,[*,‡,1c] and Glauco Tonachini[1a,d]

Contribution from the Istituto Chimico "G. Ciamician" and Istituto di Chimica Organica, Universita di Bologna, Bologna, Italy, the Department of Chemistry, Queen Elizabeth College, London, England, and the Department of Chemistry, Wayne State University, Detroit, Michigan 48202. *Received March 7, 1983*

Abstract: The [1,3] and [1,2] sigmatropic shifts of hydrogen in propene have been investigated at the MC-SCF level by using minimal and extended basis sets. A preliminary CI analysis was used to interpret the sigmatropic shifts in terms of the interaction and crossing of diabatic energy surfaces. On the basis of this analysis, transition structures were optimized at the MC-SCF level by using gradient methods and characterized by computing the Hessian matrix. The results show that the SCF level is inadequate in a large region of the potential energy surface. In particular, the [1,3] supra transition state does not exist. Of the two possible pathways toward rearrangement, the [1,2] supra transition state is ca. 10 kcal mol^{-1} lower than the [1,3] antara transition state, but both are in strong competition with dissociation.

Introduction

Sigmatropic rearrangements have stimulated a great deal of theoretical interest, and many qualitative and quantitative studies have been reported on this subject.[2-21] Much of the computational work has relied on semiempirical methods, and early investigations at the ab initio level assumed restricted geometries for the transition states.[17-21] The [1,2] shifts in closed-shell systems have been studied in more detail[22] including complete optimization and electron correlation, but only recently have calculations been reported on transition states for [1,3] and [1,5] rearrangements. The [1,3] and [1,5] shifts were fully optimized at the SCF level;[23] however, a proper description of the entire surface may not be possible at the SCF level, especially if some species have diradical character.

Propene has been chosen for the present study since it is the smallest realistic model for [1,3] sigmatropic shifts. Nevertheless, the number of valence orbitals to be considered as well as the geometric degrees of freedom make this a challenging problem with current methodology. Previous studies of this reaction by Radom and co-workers,[23] with gradient optimization at the HF/STO-3G and HF/4-31G levels, yielded two transition states for the [1,3] rearrangement. As shown in Figure 1, the "allowed" antara transition state has the migrating hydrogen located in the CCC plane with overall C_2 symmetry, and the "forbidden" supra transition state has the hydrogen positioned directly above the central carbon. The allowed and forbidden structures are nearly equal in energy, 93 and 96 kcal M^{-1} above propene with CEPA using a double-ζ+ polarization basis set.[23d] In the present paper, we have reexamined this system with MC-SCF methods to determine if transition structures persist at higher levels of theory. Computations of the diabatic energy surfaces provide an understanding of the breakdown of the SCF approach for this reaction. Transition structures for sigmatropic rearrangement have been fully optimized with a gradient procedure at the MC-SCF level.

Methods

The calculations reported in this paper were carried out at the CI and MC-SCF level with minimal (STO-3G) and extended (4-31G) basis sets. Equilibrium geometries and transition structures were fully optimized by using MC-SCF gradients[24] with both basis sets, and relative energies were recalculated using a size-consistent multireference linear coupled cluster approach[25] with the extended basis set (MR-LCC/4-31G). Integral and derivative calculations were performed by using the GAUSSIAN80 series of programs.[26] The CI and MC-SCF programs are based upon the Unitary Group method and are described in ref 27.

The CI wave function, Ψ, used in the MC-SCF approach is a linear combination of configuration state functions, Φ_k. The orbitals occurring in the Φ_k are classified as (i) core orbitals, which are doubly occupied in all configurations, (ii) valence orbitals, which have all possible occu-

Scheme I

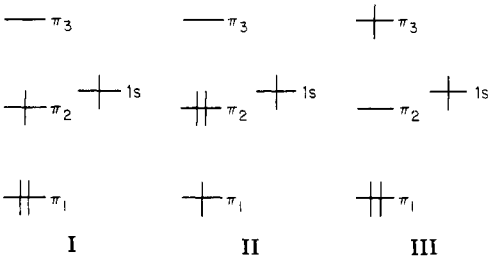

[†] Senior CIBA-GEIGY fellow (Jan-Aug 1982), Istituto di Chimica Organica, Universita di Bologna, Bologna, Italy.

[‡] Fellow of the Alfred P. Sloan Foundation, 1981-1983.

(1) (a) Istituto Chimico G. Camician and Istituto di Chimica Organica. (b) Queen Elizabeth College. (c) Wayne State University. (d) Permanent address: Istituto di Chimica Organica, Torino, Italy.
(2) Woodward, R. B.; Hoffmann, R. *Angew. Chem., Int. Ed. Engl.* **1969**, *8*, 781.
(3) Zimmerman, H. E. *Acc. Chem. Res.* **1972**, *5*, 393.
(4) Dewar, M. J. S. *Angew. Chem., Int. Ed. Engl.* **1971**, *10*, 761.
(5) Fukui, K. *Acc. Chem. Res.* **1971**, *4*, 57.
(6) Epiotis, N. D. *Angew. Chem., Int. Ed. Engl.* **1974**, *13*, 751.
(7) Berson, J. A. *Acc. Chem. Res.* **1972**, *5*, 406.
(8) Bingham, R. C.; Dewar, M. J. S. *J. Am. Chem. Soc.* **1972**, *94*, 9107.
(9) Grima, J. P.; Choplin, F.; Kaufmann, G. *J. Organomet. Chem.* **1977**, *124*, 315.
(10) Schuster, P. *Chem. Phys. Lett.* **1969**, *3*, 433.
(11) Marsh, F. J.; Thomas, B. G.; Gordon, M. S.; *J. Mol. Struct.* **1975**, *25*, 101.
(12) Kato, S.; Kato, H.; Fukui, K. *J. Am. Chem. Soc.* **1977**, *99*, 684.
(13) Carlsen, L.; Duus, F. *J. Am. Chem. Soc.* **1978**, *100*, 281.
(14) Peyerimhoff, S. D.; Buenker, R. J. *J. Chem. Phys.* **1969**, *50*, 1846.
(15) Koller, J.; Hadzi, D.; Azman, A. *J. Mol. Struct.* **1973**, *17*, 157.
(16) Peterson, M. R.; Csizmadia, I. G., unpublished results.
(17) Bouma, W. J.; Poppinger, D.; Radom, L. *J. Am. Chem. Soc.* **1977**, *99*, 6443.
(18) Meyer, R.; Ha, T. K.; Frei, H.; Gunthard, H. H. *Chem. Phys.* **1975**, *9*, 393.
(19) Karlstrom, G.; Wennerstrom, H.; Jonsson, B.; Forsen, S.; Almlof, J.; Ross, B. *J. Am. Chem. Soc.* **1975**, *97*, 4188. Karlstrom, G.; Jonsson, B.; Ross, B.; Wennerstrom, H. *Ibid.* **1976**, *98*, 6851.
(20) Isaacson, A. D.; Morokuma, K. *J. Am. Chem. Soc.* **1975**, *97*, 4453.
(21) Del Bene, J. E.; Kochenour, W. L. *J. Am. Chem. Soc.* **1976**, *98*, 2041.
(22) For a survey see Schaefer III, H. F. *Acc. Chem. Res.* **1979**, *12*, 289.
(23) (a) Bouma, W. J.; Vincent, M. A.; Radom, L. *Int. J. Quantum Chem.* **1978**, *14*, 767. (b) Bouma, W. J.; Radom, L. *J. Am. Chem. Soc.* **1979**, *101*, 3487. (c) Adeney, P. D.; Bouma, W. J.; Radom, L.; Rodwell, W. R. *Ibid.* **1980**, *102*, 4069. (d) Rodwell, W. R.; Bouma, W. J.; Radom, L. *Int. J. Quant. Chem.* **1980**, *18*, 107.
(24) Schlegel, H. B.; Robb, M. A. *Chem. Phys. Lett.* **1982**, *93*, 43.
(25) Baker, H.; Robb, M. A. *Mol. Phys.* **1983**, *50*, 1077.

0002-7863/84/1506-1198$01.50/0

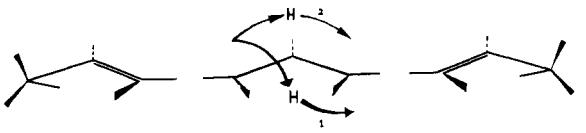

Figure 1. Antara and supra [1,3] sigmatropic shifts of hydrogen in propene (1 and 2, respectively).

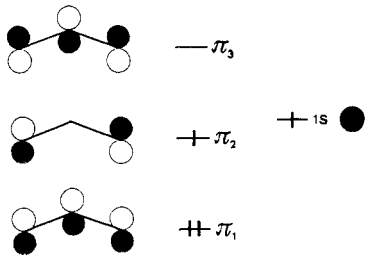

Figure 2. Valence orbitals for the allyl plus hydrogen system at infinite separation consisting of the π system of allyl and the 1s orbital of hydrogen.

pancies in the Φ_k, and (iii) virtual orbitals, which are unoccupied in all configurations. The set of configurations constitutes a full valence shell CI and hence the energy is invariant to a transformation of the valence orbital among themselves. The MC–SCF energy is optimized with respect to core-valence, core-virtual, and valence-virtual mixing, as well as with respect to the CI coefficients.

For [1,3] and [1,2] sigmatropic rearrangements in propene, the molecular orbitals can be constructed from two noninteracting subsystems, allyl radical and hydrogen atom. In the present study we have selected the three π orbitals of allyl and the 1s orbital of H for the valence space (see Figure 2). This choice is appropriate for the motions investigated since it allows proper dissociation of propene and trimethylene into allyl radical plus an hydrogen atom and also permits the correct description of a diradicaloid intermediate or transition structure. In this valence space, a complete CI for the singlet state has 20 configurations.

With the valence space defined above, calculations have been performed at three levels of approximation. First, a preliminary survey of the surface was made without detailed optimization of the orbitals or the geometry. The orbitals were obtained by orthogonalizing the MC–SCF orbitals of the noninteracting fragments. The CI coefficients were determined variationally, and the effect of orbital optimization was estimated by using second-order perturbation theory. The MC–SCF optimized geometry of the isolated allyl radical was retained for the allyl fragment. Second, full MC–SCF computations were performed with complete orbital and geometry optimization. Finally, multireference linear coupled cluster calculations were carried out by using the MC–SCF wave function as the reference space and with the core orbitals frozen.

In the preliminary calculations, our objective was to decompose the surface into diabatic components, and to relate the intermediates and transition structures to the minima and intersections of these surfaces. The wave function for each diabatic surface was built from a subset of the full CI space. A given diabatic surface can be associated with a combination of "no-bond" configurations and corresponds to a particular spectroscopic state for each of the isolated fragments.[28] To these configurations one must add charge transfer to describe bond formation. One combination of "no-bond" configurations plus related charge-transfer configurations represents a specific bonding situation and is referred to as a packet.

Results and Discussion

An MC–SCF/STO-3G computation of a planar allyl radical plus hydrogen atom at 20 Å shows that the ground state and first excited states of this system are described mainly in terms of the three "no-bond" configurations given in Scheme I. In particular, the ground state is dominated by configuration I (coefficient in the CI expansion of 0.92), while the first excited state is diradical-like and is described by an almost equal admixture of configurations II and III (coefficients of 0.66 and −0.64, respectively). As the fragments are brought together, the two diabatic surfaces are described by I or II + III plus configurations where electron transfer between "no-bond" configurations is allowed.

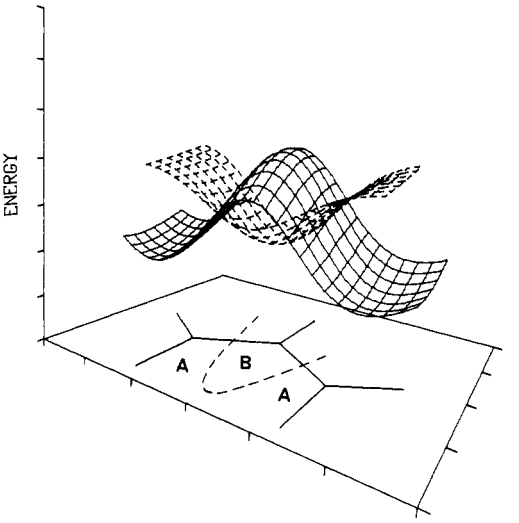

Figure 3. Intersection of diabatic energy surfaces for hydrogen moving 1.1 Å above a rigid allyl radical framework. The solid grid corresponds to the closed shell surface (packet A) and the dashed grid to the diradical surface (packet B).

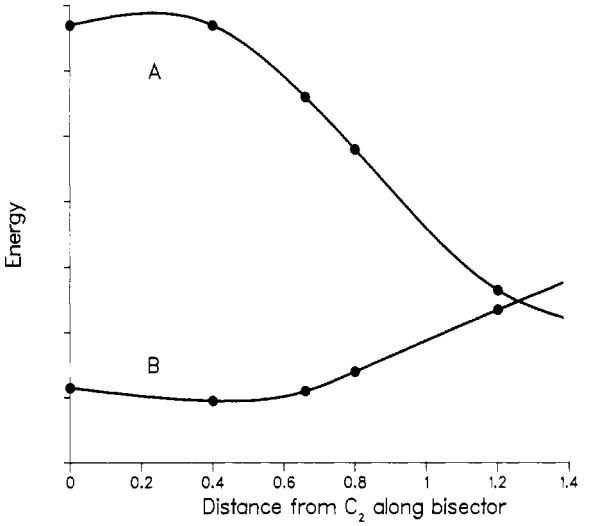

Figure 4. Cross section of the diabatic surfaces of Figure 3 in a plane containing the CCC angle bisector (closed shell A, diradical B).

Approximate Diabatic Surfaces. To obtain some preliminary information about the surface for suprafacial rearrangement, we have carried out a CI analysis of the hydrogen migration over the previously optimized allyl framework, using the orbitals obtained in the MC–SCF calculation at 20 Å. A relatively coarse grid was used and the hydrogen atom was kept at 1.1 Å above the allyl plane. The adiabatic surface corresponding to the full CI expansion has been decomposed into two diabatic surfaces, one associated with configuration I plus all related one-electron charge-transfer configurations (packet A) and the other associated with configurations II and III plus charge transfer (packet B).

As shown in Figure 3, the two diabatic surfaces intersect at almost constant energy and divide the adiabatic surface into two parts. In region A, the lowest energy is associated with configurations that describe a closed-shell propene-like structure (packet A), and in region B the lowest energy wave function describes a trimethylene-type diradical (packet B). These results suggest that the SCF level is satisfactory only in region A, while the diradical-like region B requires at least a 2 × 2 CI. Any single determinantal SCF calculation of the diradical state would be too

(26) GAUSSIAN80: Binkley, J. S.; Whiteside, R. A.; Krishnan, R.; Seeger, R.; DeFrees, D. J.; Schlegel, H. B.; Topiol, S.; Kahn, L. R.; Pople, J. A. *QCPE* **1981**, *13*, 406. STO-3G basis: Hehre, W. J.; Stewart, R. F.; Pople, J. A. *J. Chem. Phys.* **1969**, *51*, 265. 4-31G basis: Ditchfield, R.; Hehre, W. J.; Pople, J. A. *Ibid.* **1971**, *54*, 724.

(27) For details see: Hegarty, D.; Robb, M. A. *Mol. Phys.* **1979**, *38*, 1795. Eade, R. H. A.; Robb, M. A. *Chem. Phys. Lett.* **1981**, *83*, 362.

(28) Bernardi, F.; Robb, M. A. *Mol. Phys.* **1983**, *48*, 1345.

Table I. Total and Relative Energies

structure	MC-SCF/STO-3G		MC-SCF/4-31G		MR-LCC/4-31G[a]
	E_{total}[b]	ΔE[c]	E_{total}[b]	ΔE[c]	ΔE[c]
allyl radical plus hydrogen	−115.54145	0.0	−116.82125	0.0	0.0
[1,3] antara transition state	−115.52894	7.9	−116.79448	16.8	28.3
[1,2] supra transition state	−115.54757	−3.8	−116.80843	8.0	19.0
trimethylene diradical	−115.60736	−41.4			

[a] Calculated at the MC-SCF/4-31G geometry. [b] In au; 1 au = 627.51 kcal mol^{-1}. [c] In kcal mol^{-1}.

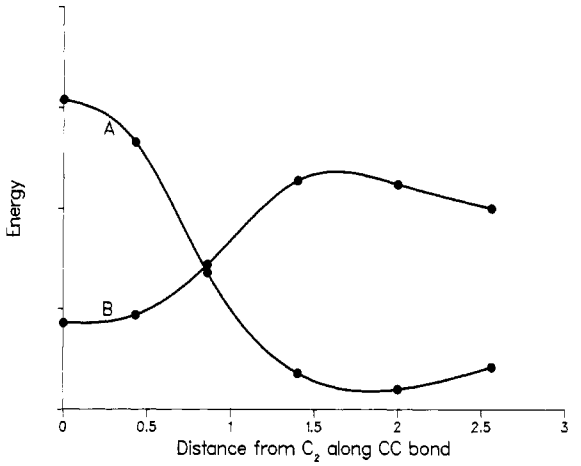

Figure 5. Cross section of the diabatic surfaces of Figure 3 in a plane containing the C_1C_2 bond (closed shell A, diradical B).

high in energy to intersect with the closed-shell surface.

Cross sections through the surfaces in Figure 3 provide more detailed information about the behavior of the diabatic energies. Figure 4 shows the variation of the energy of the two diabatic states for motion of the hydrogen in the plane bisecting the CCC angle. The diradical-like state remains lower in energy except at very large distances from the central carbon. By symmetry this crossing will also be present on the adiabatic surface. A transition state for a [1,3] suprafacial migration corresponds to a maximum for motion perpendicular to the bisecting plane and a minimum for motion within the plane. Thus the transition state can occur at the minimum in curve B, near the central carbon, or at the minimum in curve A, far from the central carbon. The latter case is well described at the SCF level and has already been shown to optimize to the antara transition state. Therefore the search for a suprafacial transition state can be confined to the region around the central carbon.

Figure 5 is a cross section of the diabatic energy surfaces for motion in a plane containing the CC bond axis. The two diabatic surfaces cross near a point above the middle of the CC bond and indicate the existence of a transition state for a [1,2] shift. Also the curves suggest that there is a minimum near the central carbon in the diradical surface. Since a [1,3] transition state must have a maximum at the central carbon for motion perpendicular to the bisecting plane, a [1,3] shift transition state perhaps does not exist.

To summarize, preliminary computations of the diabatic surfaces with the STO-3G basis predict that only the antara transition structure is well represented at the SCF level. Further, a [1,2] shift transition state is expected to be found while the supra [1,3] shift transition state found at the SCF level is predicted to be absent.

MC-SCF Geometry Optimization. In a second stage, we have used a gradient procedure at the MC-SCF level to optimize the structures suggested by the preliminary CI analysis. The geometry optimizations were performed in the complete 21-dimensional space of internal coordinates with the STO-3G and 4-31G basis sets. Each critical point was characterized by computing the Hessian for the full set of internal coordinates excluding the C–H and C–C stretches but including all of the coordinates for the migrating hydrogen, for a total of 14 degrees of freedom. The energies for the transition states are found in Table I, and the

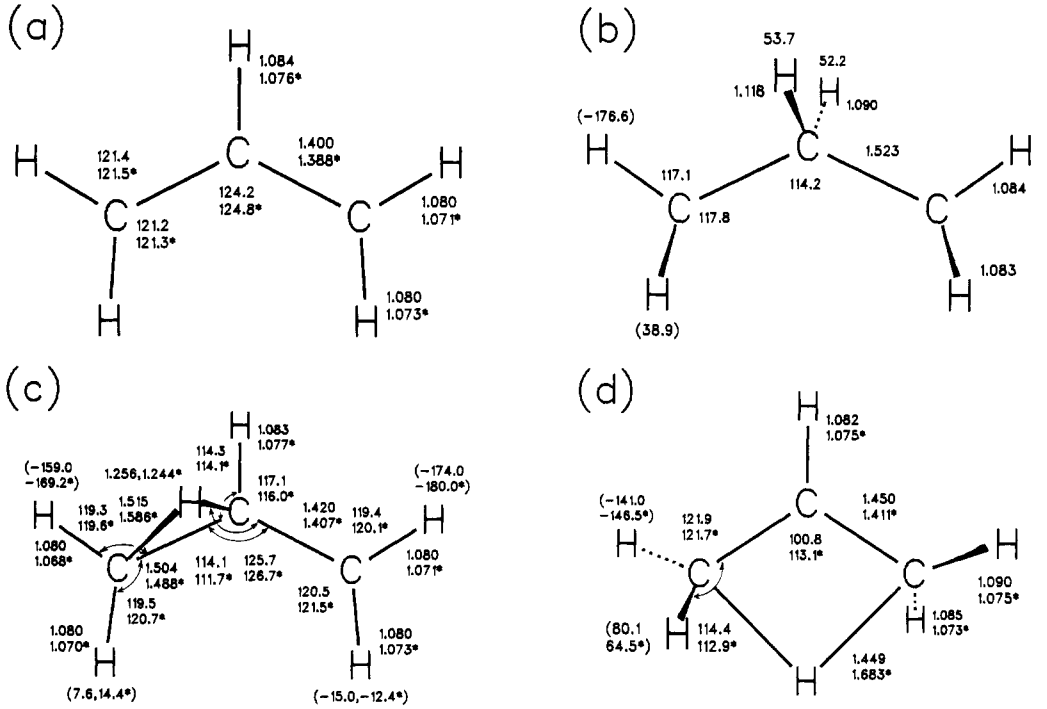

Figure 6. Optimized geometries computed at MC-SCF/STO-3G (no superscript) and MC-SCF/4-31G(asterisk): (a) allyl radical (C_{2v} symmetry), (b) trimethylene-like structure (C_s symmetry), (c) [1,2] supra transition state, (d) [1,3] antara transition state (C_2 symmetry). The HCCC dihedral angles are given in parentheses.

Table II. Energy Decomposition Analysis of Propene and the [1,3] Antara Transition State[a]

energy term	antara	propene[b]
ΔE_{deform}[c]	51.8	0.0
$\Delta E_{\text{ES+EX}}$	196.1	298.9
ΔE_{FIMC}	−244.0	−424.8
$\Delta E_{\text{CT+PL}}$	−10.9	−1.9

[a] In kcal mol^{-1} with respect to the isolated allyl radical plus hydrogen, at the MC-SCF/STO-3G optimized geometry. [b] Eclipsed conformation. [c] Energy required to distort the allyl fragment in propene to the geometry of the allyl fragment in the antara transition state.

corresponding geometries are illustrated in Figure 6.

(i) Trimethylene-Type Structure. The optimization of this structure was started at the [1,3] supra transition state found by Radom et al.,[23a] in which the migrating hydrogen is directly above the central carbon. The MC-SCF/STO-3G optimization collapses to a structure containing a central CH_2 group with nearly equal bond lengths and with a HCH angle almost bisected by the CCC plane (Figure 6b). The eigenvectors of the Hessian indicate that this is a saddle point, but not with respect to [1,3] migration. In fact, it corresponds to a transition state for disrotation of the terminal methyl groups and is a minimum in the subspace including conrotation and inversion of the terminal methylenes, ring closure, and [1,3] shift. Thus the structure is best discussed as a point on the topomerization surface of trimethylene diradical, rather than on the sigmatropic rearrangement surface of propene. Several other saddle points are likely to be found in the same region.[29-31] They are all related by internal rotation–inversion, separated by only a few kilocalories per mole, and represent minima in the subspace excluding rotation–inversion of the terminal methylenes. Since our reference space was chosen specifically to describe H migration over an allyl framework and thus is not suitable for trimethylene topomerization, these calculations were not pursued further and optimization was not carried out with the extended basis set. Several detailed investigations of the trimethylene surface have already appeared in the literature.[29-31,33]

(ii) Transition State for the [1,2] Shift. The starting point in the optimization was obtained from the preliminary CI analysis, and the final geometrical parameters computed at the MC-SCF/STO-3G and MC-SCF/4-31G levels are shown in Figure 6c. At both levels, diagonalization of the Hessian indicates that this structure is a saddle point with a single, well-defined negative eigenvalue corresponding to the hydrogen moving parallel to the C–C bond. The transition state is located very close to the intersection of the diabatic surfaces computed in the preliminary CI analysis. As expected on the basis of the Hammond postulate, its geometry is closer to trimethylene, Figure 6b, which is ca. 60 kcal mol^{-1} less stable than propene.

(iii) [1,3] Antara Transition State. The MC-SCF/STO-3G and MC-SCF/4-31G optimized geometries of the antara transition state are presented in Figure 6d. With both basis sets the Hessian matrix shows that this is indeed the saddle point for the antara [1,3] shift and that the transition vector is dominated by the hydrogen migrating from one terminal carbon to the other in the CCC plane. The MC-SCF optimized CC and $CH_{\text{migration}}$ distances are somewhat longer than the Hartree–Fock values. However, in all other aspects the MC-SCF optimized parameters do not differ significantly from those obtained at the SCF level.[23]

In the diabatic representation, the [1,2] transition state is due to the avoided crossing between the two diabatic surfaces. However, the origin of the [1,3] antara transition state is less clear. To gain some insight, we performed an MC-SCF energy decomposition analysis[28] of the barrier, similar to Morokuma's method for SCF calculation.[32] Both propene in the eclipsed conformation and the antara transition state were decomposed into the corresponding allyl radical plus hydrogen. The results are shown in Table II. The $\Delta E_{\text{ES+EX}}$ term denotes the electrostatic and exchange repulsion energy and is obtained by evaluating the energy of the system by using the MC-SCF wave function for the infinitely separated subsystems; the fragment in molecule configuration term, ΔE_{FIMC}, is the stabilization due to valence charge transfer and is obtained by a full CI in the valence space; $\Delta E_{\text{CT+PL}}$ is associated with the orbital polarization and residual charge-transfer effects (for details, see ref 28).

The decomposition shows that the deformation energy of the allyl fragment makes a large contribution to the barrier (51.8 kcal mol^{-1}). Further, the net effect of valence charge transfer in propene $\Delta E_{\text{ES+EX}}+\Delta E_{\text{FIMC}}$ = 125.9 kcal mol^{-1}) is much larger than for the antara transition state (47.9 kcal mol^{-1}). Thus one may conclude that the antara barrier has a simple interpretation in terms of a large deformation energy of the allyl fragment and much weaker bonding than propene. In contrast, the barrier for the [1,2] shift cannot be understood in these terms but must be treated as an avoided crossing.

Energies of Competing Pathways. Both the [1,2] supra and the [1,3] antara hydrogen-shift transition states in propene are comparable in energy to CH bond dissociation (Table I). The [1,3] antara transition state is calculated to be 7.9, 16.8, and 28.3 kcal mol^{-1} above allyl radical plus hydrogen atom at the MC-SCF/STO-3G, MC-SCF/4-31G, and MR-LCC/4-31G levels, respectively; correspondingly the energy of the [1,2] shift is −3.8, 8.0, and 19.0 kcal mol^{-1} relative to allyl plus hydrogen. From CEPA calculations using a double-ζ+ polarization basis set Radom et al.[23d] have also suggested that the antara transition state may be above the dissociation limit. Although these energies are sensitive to basis set size and level of correlation, it is clear that the possibility of dissociation must not be ignored when sigmatropic shifts are considered in propene. The relative energy of the [1,2] and the [1,3] antara rearrangements is much less sensitive to the calculational level. At MC-SCF/STO-3G, MC-SCF/4-31G, and MR-LCC/4-31G, the [1,2] transition state is 11.7, 8.8, and 9.3 kcal mol^{-1}, respectively, below the [1,3] antara saddle point. However, once the molecule is on the trimethylene diradical surface, ring closure will be more favorable than the additional [1,2] shift required to complete the [1,3] rearrangement.[31,33,34]

Conclusions

It is clear that the SCF level is inadequate for a study of energy surfaces whose shape is dictated by the interaction and intersection of diabatic surfaces. If a [1,3] suprafacial hydrogen migration is attempted in propene, the hydrogen crosses into a region where the trimethylene diradical is more stable and a single determinantal SCF calculation cannot describe the wave function correctly. At least two configurations are needed (II and III from Scheme I, which correlate with an excited state of allyl), and the surface computed at the MC-SCF level is dramatically different from the SCF surface. A minimum is found in the MC-SCF calculation where the SCF predicts a saddle point. Furthermore, the [1,2] shift transition structure can only be described if we take into account both of these diabatic surfaces, i.e., three configurations, I, II and III. Otherwise it does not exist. Only the [1,3] antara transition state is located on a single configuration surface where the SCF calculation is correct.

The [1,2] transition state is ca. 10 kcal mol^{-1} more stable than the [1,3] antara transition state. However, both the [1,3] antara

(29) Hay, P. J.; Hunt, W. J.; Goddard III, W. A. *J. Am. Chem. Soc.* **1972**, *94*, 638.
(30) Kato, S.; Morokuma, K. *Chem. Phys. Lett.* **1979**, *65*, 19.
(31) Doubleday, C., Jr.; McIver, J. W., Jr.; Page, M. *J. Am. Chem. Soc.* **1982**, *104*, 6533 and references cited therein.
(32) Morokuma, K. *J. Chem. Phys.* **1971**, *55*, 1236. Kitaura, K.; Morokuma, K. *Int. J. Quantum Chem.* **1976**, *10*, 326.
(33) Horsley, J. H.; Jean, Y.; Moser, C.; Salem, L.; Steven, R. M.; Wright, J. S. *J. Am. Chem. Soc.* **1972**, *94*, 279.
(34) Waage and Rabinovitch[35] reported that the activation energy for the structural isomerization of *trans*-cyclopropane-d_2 to propene-d_2 is 3.7 kcal M^{-1} higher than the geometric isomerization to *cis*-cyclopropane-d_2. The latter proceeds via the trimethylene diradical and that suggests that it lies ca. 60 kcal M^{-1} above propene and ca. 30 kcal M^{-1} below the CH dissociation limit. It is conceivable that the structural isomerization proceeds by a path not involving trimethylene, and hence may not be pertinent to the [1,2] shift transition state.
(35) Waage, E. V.; Rabinovitch, B. S. *J. Phys. Chem.* **1972**, *76*, 1695.

rearrangement and the [1,2] shift are in strong competition with dissociation. A supra [1,3] rearrangement does not appear to be possible, either as a direct shift from one terminal carbon to the other or as two [1,2] shifts. In the first case, a [1,3] supra transition structure does not exist because a diradical state is lower in energy than the closed-shell singlet. In the latter case, the topomerization via successive [1,2] shifts is unlikely because the intermediate diradical can close to give cyclopropane more easily than undergo a further [1,2] shift.[31,33]

Acknowledgment. We wish to express our gratitude to NATO (Grant RG096.81) and to the donors of the Petroleum Research Fund, administered by the American Chemical Society, for support of this work. G.T. acknowledges a computational grant from CSI-Piemonte (Torino, Italy).

Registry No. Propene, 115-07-1.

Ab Initio Heats of Formation of Medium-Sized Hydrocarbons. The Heat of Formation of Dodecahedrane

Jerome M. Schulman* and Raymond L. Disch

Contribution from the Department of Chemistry, City University of New York, Queens College, Flushing, New York 11367. *Received August 8, 1983*

Abstract: The use of ab initio molecular orbital calculations to predict accurate geometries and heats of formation has been studied for cyclohexane, cubane, adamantane, and dodecahedrane at the SCF level with use of the basis sets STO-3G, 4-31G, and 6-31G*. Good agreement with experiment is obtained for geometries in all cases. In the 6-31G* basis set, heats of formation of cyclohexane, adamantane, and cubane are in error by 0.5, 2.1, and 9.9 kcal/mol, respectively; for dodecahedrane, the heat of formation is predicted to be −5.0 kcal/mol. This work has been somewhat hampered by the unreliability of experimental thermochemical data.

Ab initio molecular orbital theory at the SCF level has been shown to be capable of the accurate prediction of geometry and thermochemistry for small hydrocarbons (C_1–C_7). These predictions require full geometry optimization at basis set levels of split valence or double-ζ (with d orbitals on all carbon atoms if there is appreciable strain energy)[2] and the construction of isodesmic[3] or preferably homodesmic[4] thermochemical processes. All this notwithstanding, the application of these methods to hydrocarbons through C_7 will soon become routine.

The present work attempts to assess the feasibility of applying these methods to the larger systems cubane, adamantane, and dodecahedrane. The latter is of particular interest, because semiempirical molecular orbital[5] and molecular mechanics[6] methods yield substantially different ΔH_f^{298} values. One conclusion of this study is that the accuracy of calculated heats of formation is strongly dependent upon the quality of available zero-point energies, heat capacity data, and experimental heats of formation for species involved in a homodesmic reaction.

Methods

The ab initio calculations were performed by optimized programs developed by us (The Queens College Quantum Chemistry Package). The basis sets employed are STO-3G,[7a] 4-31G,[7b] and 6-31G*.[7c] For dodecahedrane, the 6-31G* energy was estimated by a procedure described below.

The ΔH_f^{298} for cubane, adamantane, and dodecahedrane are calculated from several homodesmic reactions. Heats of reaction at 0 K are computed from the ab initio energy differences corrected for zero-point energies. In the absence of experimentally determined vibrational frequencies by which the latter could be calculated, values obtained from molecular mechanics are used. Enthalpies are converted from 0 K to 298 K according to the equations of Hehre et al.[3] In the final step, the desired ΔH_f^{298} is obtained from these heats of reaction corrected to 298 K and the experimental ΔH_f^{298}.

Results

Table I contains the ab initio and zero-point energies for ethane, propane, isobutane, cyclobutane, cyclohexane, cubane, adamantane, and dodecahedrane; their ΔH_f^{298} and enthalpy corrections from 0 K to 298 K are also included. All species are treated as ideal gases. The ab initio energy for each basis set corresponds to the geometry optimized in that basis with the sole exception of the 6-31G* energy of dodecahedrane, which is estimated as the sum of the 4-31G energy and a correction of 0.05645 au per carbon atom—one-fifth of the difference between the energies of planar cyclopentane in the two basis sets. This correction, nearly identical with that recommended by Hehre and Pople,[1d] is probably suitable for molecules with little angle strain. When applied to adamantane, it furnishes a 6-31G* estimate of the energy only 1.3 kcal/mol too high, whereas for cubane the error is 8.4 kcal/mol.

Table II contains the optimized geometric parameters for cyclohexane, cubane, adamantane, and dodecahedrane. The geometries in the various basis sets are very similar and in good agreement with experimental values. For cubane, the calculated geometries compare well with previous STO-3G and 4-31G values,[8a,b] as well as recent "double-ζ + d" results.[8c]

Table III contains the calculated values of ΔH_f^{298} for cyclohexane, cubane, adamantane, and dodecahedrane in the STO-3G, 4-31G, and 6-31G* basis sets, which were obtained from the seven

(1) For recent examples, see: (a) Wiberg, K. B.; Wendoloski, J. J. *J. Am. Chem. Soc.* **1982**, *104*, 5679. (b) Wilberg, K. B. *Ibid.* **1983**, *105*, 1227. (c) Schulman, J. M.; Disch, R. L.; Sabio, M. L. *Ibid.* **1982**, *104*, 3785. (d) Hehre, W. J.; Pople, J. A. *Ibid.* **1975**, *97*, 6941.
(2) Binkley, J. S.; Pople, J. A. *Chem. Phys. Lett.* **1975**, *36*, 1.
(3) Hehre, W. J.; Ditchfield, R.; Radom, L.; Pople, J. A. *J. Am. Chem. Soc.* **1970**, *92*, 4796.
(4) (a) George, P.; Trachtman, M.; Beck, C. W.; Brett, A. M. *Tetrahedron*, **1976**, *32*, 317. (b) George, P.; Trachtman, M.; Brett, A. M.; Bock, C. W. *J. Chem. Soc., Perkin Trans. 2* **1977**, 1036. We suggest use of the term "homodesmic" to replace "homodesmotic".
(5) Schulman, J. M.; Disch, R. L. *J. Am. Chem. Soc.* **1978**, *100*, 5677.
(6) (a) Engler, E. M.; Andose, J. D.; Schleyer, P. v. R. *J. Am. Chem. Soc.* **1973**, *95*, 8005. (b) Allinger, N. L. *Ibid.* **1977**, *99*, 8127.
(7) (a) Hehre, W. J.; Stewart, R. F.; Pople, J. A. *J. Chem. Phys.* **1969**, *51*, 2657. (b) Ditchfield, R.; Hehre, W. J.; Pople, J. A. *Ibid.* **1971**, *54*, 724. (c) Hariharan, P. C.; Pople, J. A. *Chem. Phys. Lett.* **1972**, *16*, 217.

0002-7863/84/1506-1202$01.50/0